JOURNAL OF SPACECRAFT AND ROCKETS
Vol. 41, No. 1, January–February 2004

Space Test of Sensor-Fused Telerobotics for High-Precision Tasks

Kazuo Machida*
University of Tokyo, Tokyo 113-8656, Japan

An evaluation of the world's first precise extravehicular robot boarded on the Engineering Test Satellite-VII is presented. The concept of sensor-fused telerobotics that has the dual-loop structures of multisensory autonomous control and active sensing of work environment was applied to perform high-precision tasks under the space specific conditions of low-bandwidth communication link, time delay, work-environment uncertainties, and insufficient visibility from onboard cameras. The robotic system features dexterity, autonomy, and telesensing capability using a three-finger multisensory hand at a work site in space and flexible operability using a computer-graphics-based human/robot interface with a virtual hypercamera at an operation site on the ground. The robot was operated for two years, and the sensor-fused telerobotics technology was demonstrated to be applicable in space.

Nomenclature

F	=	force detected by force/torque sensor
M	=	moment or torque detected by force/torque sensor
x, y, z	=	position elements in Cartesian coordinate, where z is axial direction of hand

Introduction

SPACE robots that perform delicate, complex tasks in unmanned facilities will be indispensable in the near future. One of the key technologies is telerobotics using a hand with dexterity and autonomy. To date, no such robotic system has been developed for space extravehicular applications. In 1993 the Robot Technology Experiment was carried out on the Space Shuttle.[1] However, it was an intravehicular robot with a one-degree-of-freedom (DOF) multisensory gripper operating in a Spacelab rack. In 1994 a flight test of a force/torque (FT) sensor built at the Jet Propulsion Laboratory, Pasadena, California, was carried out on the Shuttle Remote Manipulator System; data available online of http://ranier.hg.nasa.gov/telerobotics_page/Technologies/0202.html [cited 10 July 2002]. The small arm of the Japanese Experiment Module[2] to be onboard the International Space Station will also use a one-DOF tool with a FT sensor as an end effector. Recently, a self-adaptive and reconfigurable hand,[3] which consists of three underactuated fingers, has been developed to extend the capability of the Special Purpose Dexterous Manipulator.[4] ESA has developed a medium-size dexterous robot arm for the External Use of Robotics for Payload Automation mission.[5] Many studies on advanced telerobotics have also been carried out.[6] However, most of them lack dexterity and autonomy because of the limitations of DOF and sensors of the hand.

The Ministry of Economy, Trade, and Industry of Japan has developed a precise space telerobotic system, called Advanced Robotic Hand System (ARH), which increases dexterity and autonomy by using a three-finger multisensory hand. ARH was launched on Engineering Test Satellite-VII (ETS-VII)[7] in November 1997, and a two-year flight test was performed. ARH became the first telerobot working in an extravehicular space environment to perform high-precision tasks on small parts. The author, a principal investigator on the project, proposed the concept of sensor-fused telerobotics as an expansion on Sheridan's telerobotics concept,[8] using multisensory information obtained at the work site in space as well as at the operation site on the ground. This paper first presents the concept of sensor-fused telerobotics. Then, remote skill, autonomy, and telesensing by the hand are described. Next, a human/robot interface utilizing multisensory information is described. Finally, the robot operations performed on ETS-VII are evaluated.

Received 7 August 2002; revision received 22 April 2003; accepted for publication 2 May 2003.

*Professor, Department of Aeronautics and Astronautics, 7.3.1 Hongo, Bunkyo-ku. Senior Member AIAA.

Sensor-Fused Telerobotics to Cope with Space Specific Issues

There are three issues in telerobotic operation for precise in-orbit servicing: precision, uncertainty, and complexity. Precise teleoperation from the ground is extremely difficult because of time delay, low-bandwidth communication, and the lack of camera images near the objects. The efficiency of teleoperation drastically decreases with increases in required precision and time delay. Therefore, some autonomous skills are necessary. The second issue involves the accumulation of geometric error. Most servicing tasks change the work environment with time. Because the errors of the geometrical model thus accumulate, interactive measurement must occur with the task. The third issue is the increase in the operation DOF and monitoring sensor information required for carrying out precise tasks. In general, a space robot uses multieffectors, such as a mobile unit, an arm and fingers, to execute high-precision tasks in a wide working area. A ground operation system must reduce the operator load in spite of increasing the operation DOF and monitor information.

The sensor-fused telerobotic structure shown in Fig. 1 addresses these issues. For precise manipulation a three-finger multisensory hand uses its fine mechanisms with multisensor-based control. To address geometric uncertainty, an interactive sensing loop uses multisensors. We use here the term "telesensing" for active and interactive sensing to learn the geometric properties and state of objects in space. To address interface complexity, a desktop "sensor-fused telerobotic" interface provides a unified environment of multieffector operation and multisensor monitoring.

Remote Skill, Autonomy and Telesensing by Multisensory Hand

Three-Finger Multisensory Hand

A multisensory hand is a key component of our system. Figure 2 shows the developed flight model. The hand for space applications especially requires simple and reliable mechanisms that have precise controllability without an increase in the load of the control computer and have grasping robustness. To meet these requirements, we devised three mechanisms: a hybrid three-finger module, a compliant fingertip, and a wrist compliance device, as shown in Fig. 3. The hybrid finger module has one linear motion finger A and two rotation fingers B and C. Because each finger has one DOF, the hand has three DOF in total. Each rotation finger has an L-shaped link where strain gauges are fitted for measuring contact and grasp force. Fingers B and C move in the position-control mode, and finger A

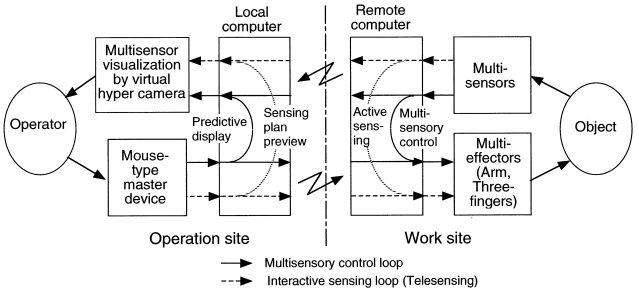

Fig. 1 Structure of sensor-fused telerobotics.

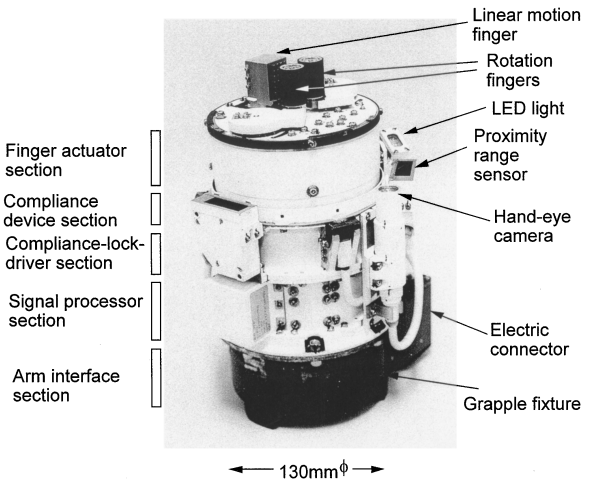

Fig. 2 Flight model of three-finger multisensory hand.

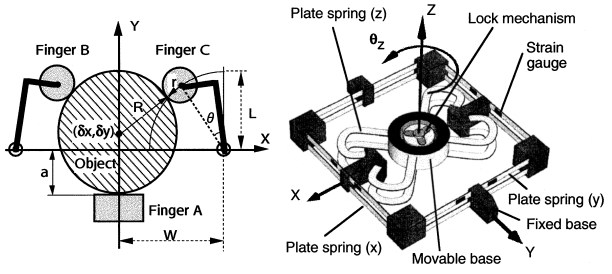

Fig. 3 Schematic of hand mechanism: left, hybrid finger module; and right, wrist compliance device with lock mechanism.

moves in the force-control mode. Finger A has a compliant fingertip composed of a pin array preloaded with springs that enables the finger to grasp various objects fitting its shape.

A wrist compliance device is devised to compensate the positioning error of the arm and also to absorb stress during impact. It features compactness and lock capability. The movable base on which the finger module is mounted is suspended by plate springs, which provide compliance with respect to x, y, z, and roll axes. This device compensates the position error of 1.5 mm and the rotation error of 2 deg. A lock mechanism in the device rigidizes the movable base during arm motion to suppress vibration.

Five kinds of sensors are installed around the hand, namely, a hand-eye camera, three proximity-range sensors, a pair of grip force sensors, a compliance sensor to measure fine displacement, and a wrist FT sensor. Three range sensors of the LED/PSD (laser-emitting diode/position sensing device) are equally spaced around the housing of the hand. A red LED array microlamp is attached for work during an eclipse. The sensor signals are preprocessed and converted to the serial signal at the signal processor section. The hand has a standardized grapple fixture with an electric connector to connect with various space robotic arms. The hand was used by two robot arms in the space test.

Strategy for Multisensor-Based Control

Figure 4 shows the basic control strategy to overcome the difficulty of ground teleoperation caused by time delay and low bandwidth. Most tasks can be decomposed to the processes of search, position estimation, relative navigation, grasping, and manipulation. Contact and noncontact sensors are applied hierarchically. First, the robot searches for the object by scanning with the range sensor and/or the hand-eye camera. Second, it determines the position or size of the object by noncontact sensing. Accurate local coordinates on the task plane can also be generated by sensor-fused measurement using the range sensors for vertical axis and the hand-eye camera for in-plane axes. Third, the relative navigation of the arm in the local coordinates is conducted under monitoring by an external monitor camera and a wrist FT sensor. Fourth, the contact sensor-based compensation is executed. Before grasping the object, position compensation is carried out through contact point sensing using the grip force sensors. Precise position adjustment of the arm is also executed through displacement sensing by the wrist compliance device. The robot then grasps the object firmly under grip force control and manipulates it under wrist force control.

While transporting the object, the robot searches for the destination by noncontact sensing. Position and alignment of the arrival port are identified by processing images and ranges.

Telesensing of Uncertain Work Environment

A common understanding of the object/environment by the robot and the human operator is indispensable for interactive telesensing to overcome the uncertainties. Figure 5 shows the basic strategy for gaining such a common understanding. For close-up-front viewing local vertical adjustment of the hand-eye camera axis by range measurements and image data acquisition are conducted. For cross-sectional viewing the range sensor is scanned, and then the depth profile is acquired. Uncertainties of the noncontact sensing measurement are improved by contact sensing. Using the grip-force

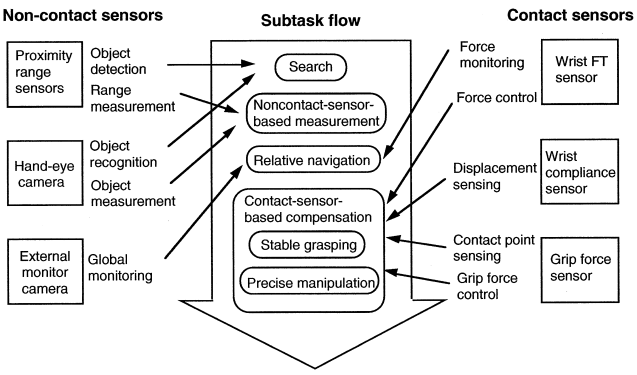

Fig. 4 Basic strategy for precise task execution using multisensors.

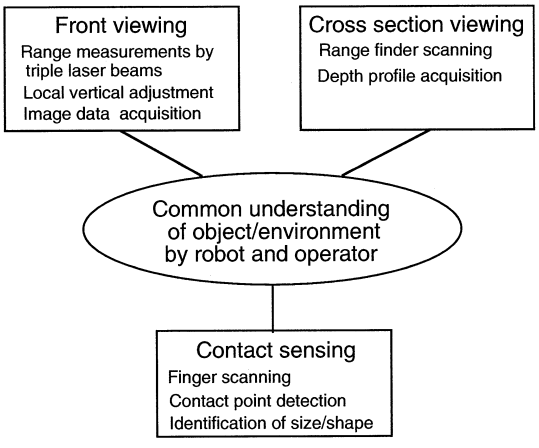

Fig. 5 Basic strategy for telesensing.

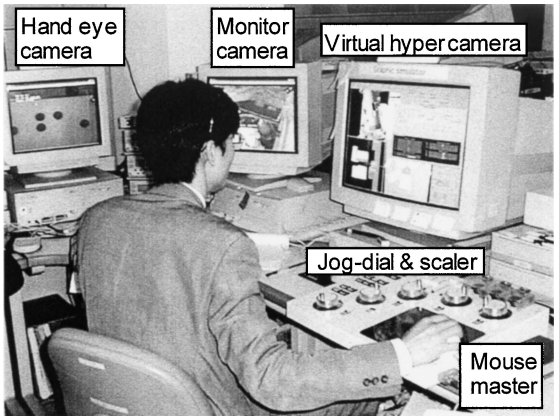

Fig. 6 Desktop ground operation system.

sensors and finger joint sensors, the fingers work like a pair of vernier calipers. In telesensing, sensor data are fused in the ground computer with intervention by a human operator.

Ground Operation System

We developed a desktop human/robot interface to reduce operator workload as shown in Fig. 6. It features a mouse-type master device, a virtual hypercamera, and teleteaching. An operator sees the views of the hand-eye camera, monitor camera, and virtual hyperrcamera, but mainly uses the virtual hypercamera view during operation.

Mouse-Type Master Device

In precise teleoperation we must operate multieffectors as the arm and fingers. We developed a mouse-type unilateral master device in order to operate them by means of one device. The mouse directs displacement of the arm position in a two-dimensional plane, which can be selected and changed arbitrarily according to the situation. Three switches embedded in the head of the mouse direct the motion of the three fingers. Furthermore, the master device is more suitable for our Graphical User Interface (GUI)-based desktop interface, than a conventional joystick.

Virtual Hypercamera

We developed a software camera to monitor the robot working state in detail. It generates images from the multisensor's telemetry data on the basis of a geometrical model. We call it a "virtual hypercamera" because the images are generated using real data. It provides a view from any angle and zooming and displays various important information unobtainable by a real camera. Figure 7 shows an example of its display. It provides 1) superimposed display of real and virtual-hypercamera image, 2) bird's eye view of the robot, front view and side view of the fingers, 3) auxiliary lines (tip and center line of the hand, work coordinate, etc.), 4) virtual geometrical guides such as cone and pipe, 5) virtual plane generated from the distance measured by the range sensors, 6) range sensor laser beam, and 7) force vector of wrist and fingers.

The virtual hypercamera requires much less data than a real camera, thus it is suitable for monitoring a far-distant space robot over a low-bandwidth communication link, and it is also useful in the case that a real camera view cannot be obtained. We use it in operation where the camera view is not available and in eclipse.

Teleteaching

We are also able to teach the arm motion remotely using the mouse-master device. The method is based on a prior work of the author.[9] An operator teaches simple tasks by dragging and dropping a graphic tag attached to the finger by the mouse. An animation of the taught motion is reproduced on the display to check safety and then the verified motion is replayed in space. The force is controlled by preset force command. This seamless operation of teaching, preview, and execution using the virtual-hypercamera display is very effective in telesensing uncertain objects and anomaly examination in space as described later.

Table 1 Specifications of telerobotic system

Item	Specification
Total system mass	45 kg
Dimensions (stowed)	500 × 480 × 480 mm
Average power	80 W
Hand	
DOF	3
Grip force	30 N
Compliance	0.15 mm/N (x, y) 0.075 mm/N (z) 3 deg/Nm (roll)
Miniarm	
DOF	5
Length	716 mm (from base to hand)
Accuracy (relative)	±0.5 mm, ±0.3 deg
Tip force, torque	40 N, 7 Nm
Torque driver	1.4 Nm/2.25 rpm
Telemetry/Command	
Teleoperation command	200 bits × 4 Hz
Packet telemetry	12 kbps
Video Data (down link)	
Channel	2ch, JPEG compressed monochrome
Frame rate	2frame/s
Mission period	1.5 years

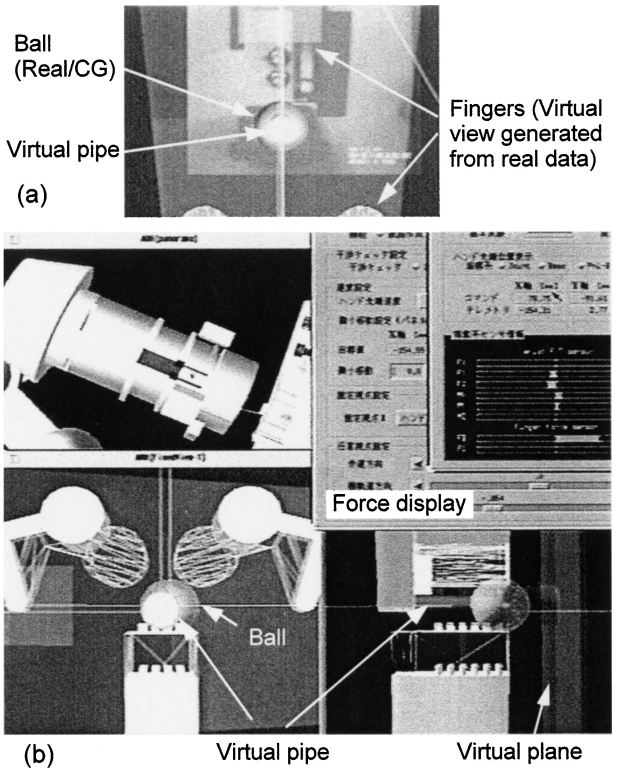

Fig. 7 Example display of virtual hypercamera: a) superimposed display of CG and video image and b) bird's eye view, front view, side view, and bar graph.

Space Test on ETS-VII

ETS-VII flies in a circular orbit at an altitude of 550 km and an inclination of 35 deg. It consists of the chaser satellite named Hikoboshi (Altair in English) and target satellite named Orihime (Vega). ARH is boarded on the earth facing plane of Hikoboshi. Table 1 lists the specifications of the ARH. Figure 8 illustrates the overall system for the space test. The robot unit constitutes the hand, a human-sized arm, a hand exchange platform, and a taskboard. The space test is carried out using the stand-alone and the long-arm connect configurations. In the stand-alone configuration the robot system executes the tasks using the taskboard attaching the hand

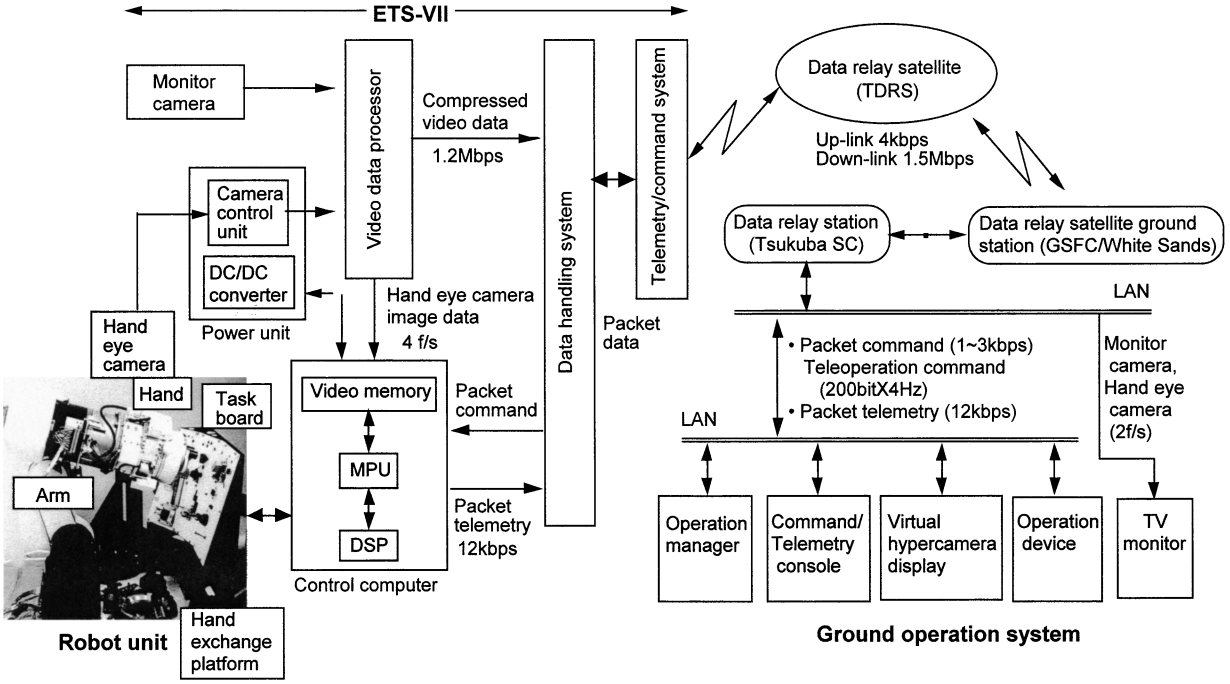

Fig. 8 Communication signal flow of whole telerobotic system.

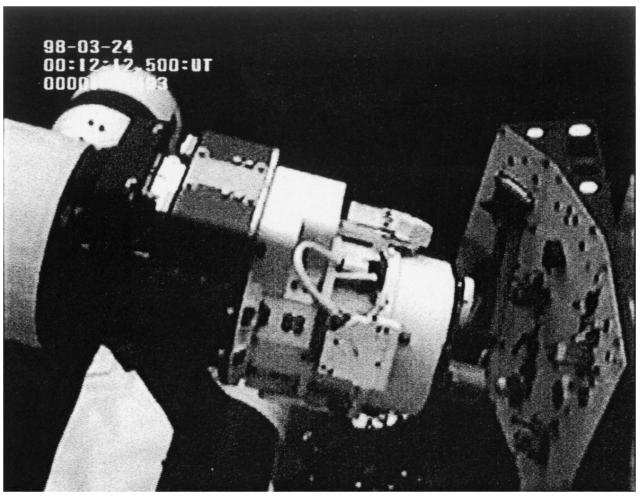

Fig. 9 View of robot in space.

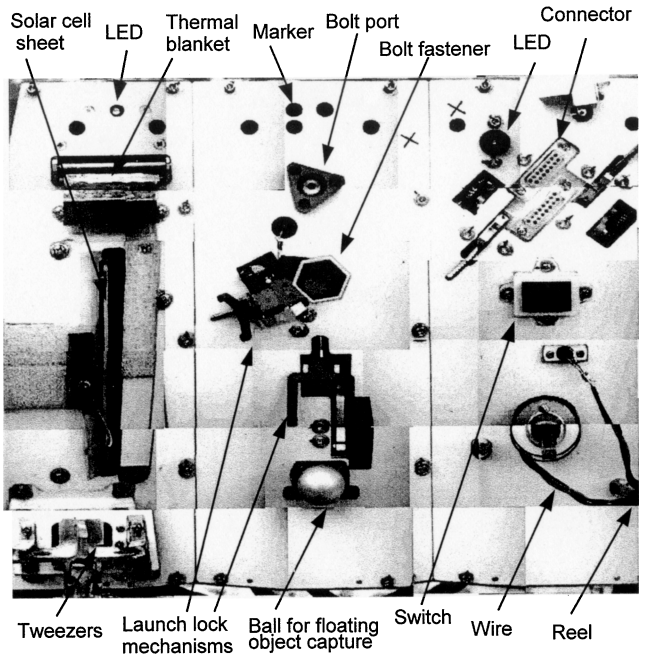

Fig. 10 Panoramic view of taskboard on Hikoboshi.

to its own human-sized arm. In the long-arm connect configuration the hand is removed and connected to the long-arm developed by National Space Development Agency of Japan,[5] and servicing tasks for a small task panel onboard Orihime are performed.

Communication between the ground system and ETS-VII is linked via Goddand Space Flight Center, Greenbelt, Maryland, White Sands, New Mexico, and the Tracking and Data-Relay Satellite (TDRS). On average, a total time delay from 5 to 7 s is measured between the space robot and the ground system. The communication period between ETS-VII and TDRS is about 42 min per revolution. A robot operation time of 20 min is allotted in this duration. Onboard software is uploaded from the ground according to the experiment.

The hand-eye camera takes close-up views of work objects for vision-based control. Overall views of the robot are taken by a monitor camera. Both cameras are monochrome, and video data are sent to the ground after JPEG compression.

The first critical event was to construct the robot to work configuration, releasing the arm from the latch mechanisms and connecting the hand fixed on the hand exchange platform. Figure 9 shows the work configuration in space. The many parts with lock mechanisms are attached to the taskboard for the space test. Figure 10 shows the panoramic view of the taskboard taken by the hand-eye camera. Table 2 summarizes the robot tasks and results of the space test. The pictures and movies can be seen on line at http://www.rosetta.t.u-tokyo.ac.jp/ARH/ARHEng/[cited 10 July 2002]. The main results are evaluated next.

Sensor-Fused Measurement

Automatic local coordinate generation by sensor-fused measurement using the range sensors and the image sensor was evaluated. The local vertical axis perpendicular to the panel was obtained so that all distances could be made identical, using the range sensors. Then, the image of two round marks (8 mm diam) was taken by the hand-eye camera and was processed. Because the line connecting

Table 2 Summary of space test results

Experiment items	Outline of tasks	Results
Stand-alone mode		
Connector mate/demate	Connecting/disconnecting an electrical plug and switching a LED indicator	Success in autonomous mode: Precise task within 0.5 mm accuracy was demonstrated. Misoperation in teleoperation mode
Bolt fastener mate/demate	Remove bolt by unscrewing, then mate and screwing	Success in autonomous mode Success in teleautonomous mode
Solar-cell sheet handling for power generation	Drawing and stretching a solar-cell sheet and a blanket from drums, and sticking on a panel for solar-power generation	Success in autonomous mode: Handling tasks for flexible sheets, tweezers, and power generation were demonstrated.
Wire handling	Manipulating a peg with a wire and wrapping the wire around reels	Success in teleoperation mode: Handling of flexible wire by teleoperation from the ground under time delay was demostrated.
Working in eclipse	Connecting an electrical plug in eclipse by the aid of LED illuminator and virtual hyper camera	Success in autonomous mode: Effectiveness of virtual hypercamera and LED illuminator in eclipse were demonstrated.
Floating object capture	Grasping a floating small ball	Failure: The small ball could not float because of failure of tether mechanism
Long-arm connect mode		
Connector mate/demate	Connecting/disconnecting an electrical plug on a target satellite	Success in autonomous mode: Error compensation of a long arm by the multisensory hand was demonstrated.
Sample retrieval	Inspecting a task panel on a target satellite Orihime and retrieving a sample cylinder to a chaser satellite Hikoboshi	Success in autonomous mode: Sensor-fused telerobotics including telesensing under uncertain work environment was demonstrated.

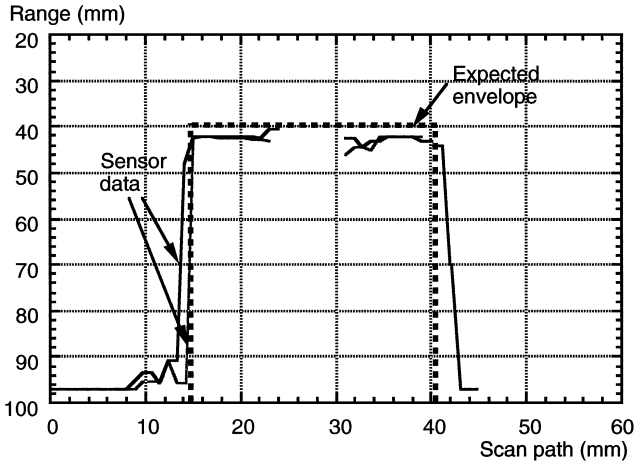

Fig. 11 Depth profile of sample cartridge measured by proximity range sensor.

the two marks represents the unit vector of the y axis, the local coordinates x, y, z were obtained. We could acquire the local coordinates within an accuracy of 0.9 mm and 0.2 deg under various sunlight conditions. This is a more accurate result than that obtained by the conventional method using only image processing.

We also measured some parts by telesensing on the basis of the strategy depicted in Fig. 5. For a hexagonal cylinder sample onboard Orihime, the hand-eye camera was used for front viewing, and then cross-sectional viewing was achieved by scanning it with the range sensor, as shown in Fig. 11. Next, the contact sensing was used to estimate the center position of the cylinder from the opening angle of the fingers while detecting the contact force by gradual closing of the three fingers. On the ground virtual hypercamera images that generated from the telemetry data of finger angles were monitored as shown in Fig. 12. When the object was grasped lightly at the initial step, a large imbalance was seen in the opening angle of the fingers (Fig. 12a), and it was evident that there was a large difference between the part position displayed based on the CAD data and the actual position. After estimating the position from the opening angle of the fingers, grasping was done again, with relative movement of the hand according to the difference. From the angle of the fingers, it was evident that the hand was positioned around its center axis (Fig. 12b). A few errors were calculated again at this time, and the CAD data were corrected. Finally, a position correction of 9 mm was made, and the actual state in space and the geometric model on the ground were completely matched (Fig. 12c). The accuracy of calibration by this method is evaluated to be within 1 mm.

Image Processing at Noon and Night

Position measurement by image processing without marks is also important. An important point is that the sunlight condition varies from moment to moment in a low Earth orbit. The illumination difference between sunlight at noon and the LED red light of 1 W at night exceeds the regulation range of an electronic shutter. So, we employed an optical filter to eliminate all light except the red band. Figure 13 shows the receptacle images taken during satellite day and night. Clear images were obtained in both cases.

The position and orientation of the receptacle were measured by processing the pinhole image. Lighting direction changes and reflection properties also make image processing difficult. We apply the feature extraction method based on the geometrical properties of the receptacle to reduce the influence of such disturbances. The measurement was carried out within the accuracy of 0.9 mm for position and 0.6 deg for orientation. The measurement under the LED illumination in eclipse was always successful. However, in the daytime we sometimes encountered image-processing failure during the feature extraction of the pinhole image, as a result of the relatively small number of pixels of a metallic pinhole (50–100 pixels/hole) and large variation of the sunlight condition. An adaptive algorithm to acquire the optimum threshold will be needed for feature extraction under minute illumination changes.

Sensor-Fused Operation for Bolt Fastener Mate/Demate

As an example of precise task execution by sensor-fused telerobotics, a bolt fastener mate/demate is described. An operator cannot see the bolt fastener and port clearly from the monitor camera. According to the basic strategy shown in Fig. 4, the robot searched for a bolt head and a pair of reference marks near the bolt by means of the hand-eye camera. Generating local coordinates based on the marks, the hand approached the bolt head by relative navigation. For screwing the bolt the hand must grasp the bolt head so as to match its alignment and position to the bolt center axis accurately. Misalignment of the vertical axis was corrected using the range difference,

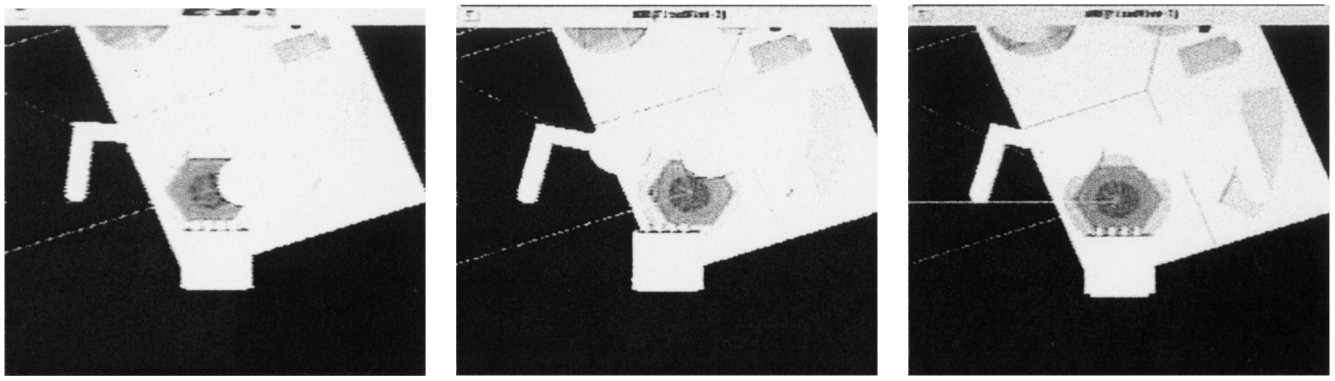

a) b) c)

Fig. 12 Remote measurement of sample position by grasp-sensing from the ground: a) initial grasping, b) second grasp sensing, and c) third grasping after calibration.

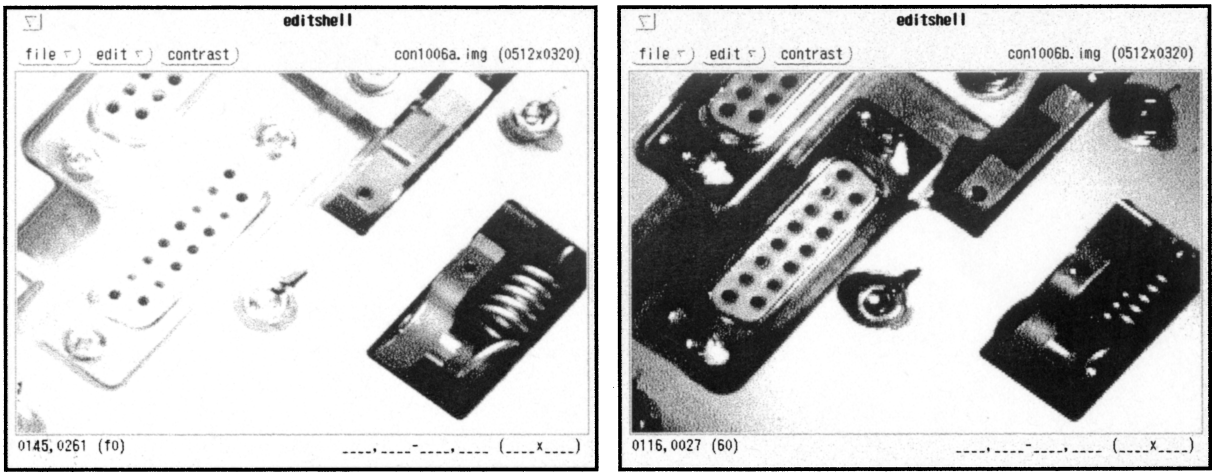

Fig. 13 Image of D-sub receptacle: a) albedo illumination in daytime and b) LED illumination in eclipse.

and the position was precisely corrected by finger contact sensing. Thus, centering was completed, and the fingers grasped the bolt head without misalignment.

Next, the wrist roll axis was rotated by steps of 60 deg to remove the bolt. Figure 14 shows the data compared with the ground-test data. After turning to 180 deg, the bolt was pulled up within the movable range of the compliance device to judge based on the reaction force whether it was removed. Because the force was detected, the robot proceeds to the next 180-deg rotation. The robot removed the bolt by repeating the same operation. In this phase the robot performed the task autonomously.

Then, bolt mating and screwing to another port were performed in the mixed mode of teleoperation and autonomous control. The horizontal position adjustment to the port center was executed under autonomous control using the sensor-fused measurement. After mating with the port, only the wrist rotation axis was teleoperated from the ground so as to manage the torque manually. The operator screwed the bolt by rotating the jog-dial, monitoring the bar graph of the FT sensor data on the display. The arm was controlled in force control mode for insertion axis and compliance control mode for other axes during screwing. The sensor-fused telerobotics has enabled this task to be completed within 20 min, which was impossible in conventional teleoperation.

Figure 14 reveals some interesting points. The robot proceeded through the task similarly for both space and ground. This means the multisensory control worked robustly. FT sensor data show the bolt unscrewing was smoothly executed with small friction in space. On the other hand, large disturbance of force and moment is observed on the ground as a result of gravity. Therefore, it is noted that the weightless environment in space is suitable for force-sensor-based control.

Sample Retrieval from Target Satellite Under Uncertain Condition

In this experiment the hand is removed from the human-sized arm and connected to the 2.4-m-long arm. Assuming the Orihime as a material experiment satellite, the robot removes the sample from a cell on Orihime, and then places it in the port on the Hikoboshi, while the two satellites are docked together. The sample and its storage cell are illustrated in Fig. 15. Three pins are arranged in the radius direction in the cell hole, and corresponding hook-shaped guide slot are cut on the side of the sample cylinder. To remove the sample, the robot must push the sample along the latch slots against the spring, then rotate it 60 deg counterclockwise, and then pull it out along the guide slot. This is a very difficult task because the positioning accuracy of the long arm is insufficient to handle the sample. Moreover, the monitor camera view of sample cell and recovery port are obstructed. To overcome these difficulties, we use the functions of multisensory control and telesensing.

Figure 16 shows scenes of the operation. The sample cannot be viewed from the monitor camera during grasping, and thus the virtual hypercamera is essential (see left of Fig. 16). First, the sample position and depth profile were detected by telesensing. Then the sample was grasped, and the center position of the hand finely adjusted by the contact sensing (see Fig. 12). The grasping depth along the z axis was adjusted based on the range sensor measurement. Then, the sample was firmly grasped. Next, the sample was pulled up under force control ($Fz = 7$ N) to check the lock status. Then, the sample was rotated 60 deg counterclockwise under pushing by force control ($Fz = -10$ N), and then lifted up by force control ($Fz = 5$ N), thus completing sample removal. Figure 17 shows the data of hand position and wrist force during the task. The sample was then transported to the Hikoboshi recovery port and fixed to it (see Fig. 16c).

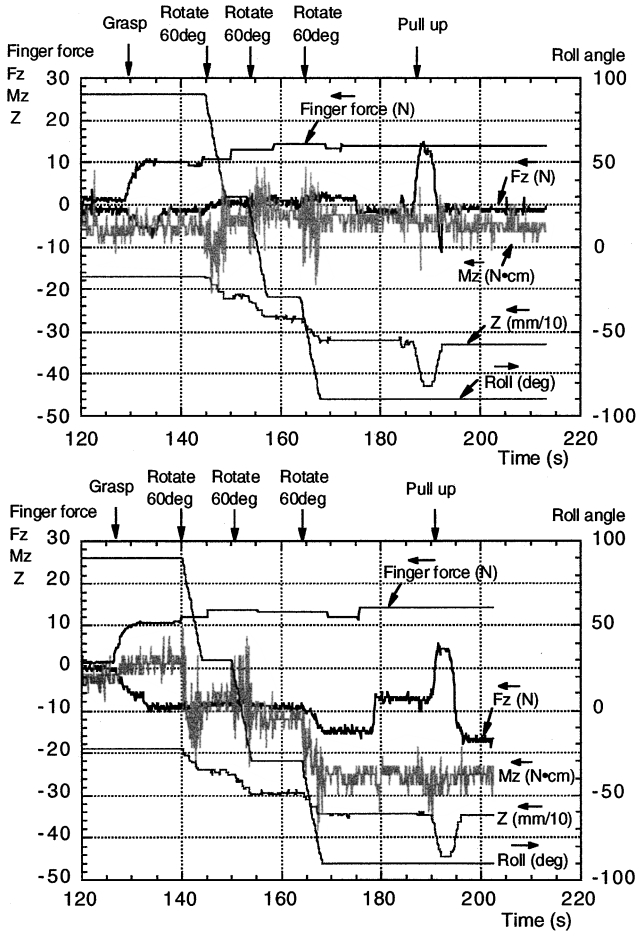

Fig. 14 Multisensory control data in bolt unscrewing: top, space and bottom, ground.

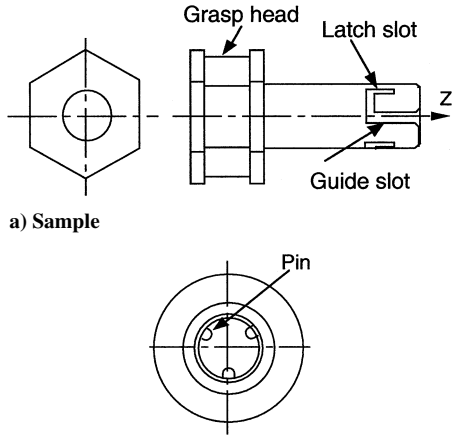

Fig. 15 Schematic of sample cartridge and sample cell.

On the ground, judging the overall state of operation on the basis of virtual hypercamera image of CG produced from the telemetry data, the operator decided Go/No-Go for supervisory control of each task.

Evaluation of Other Tasks

We carried out a solar-cell installation experiment.[10] In this experiment the robot pulls out an amorphous solar-cell sheet wound around a drum, stretches, and then attaches the sheet to the panel by a Velcro™ fastener autonomously. The hand grasps a rubber grip fixed to the end of the sheet with Velcro. In the first trial the robot aborted the task because the rubber grip stuck on the task board

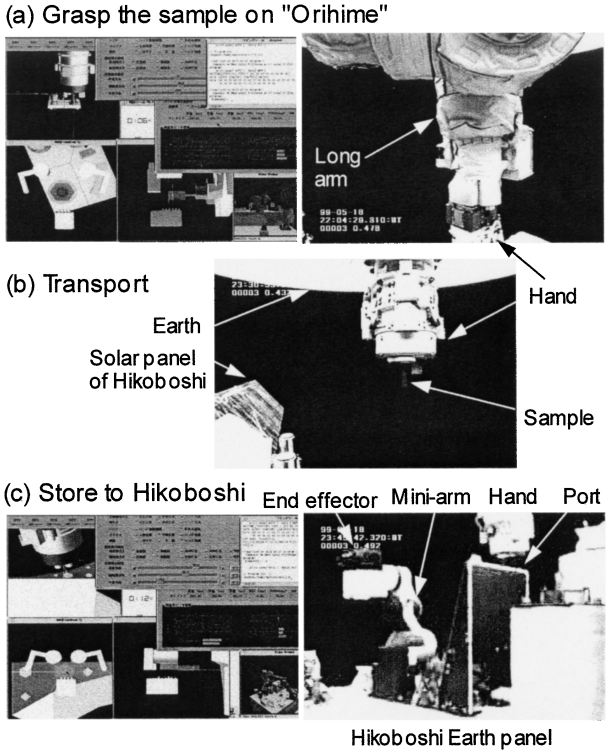

Fig. 16 Operation scene in sample retrieval from Orihime to Hikoboshi: virtual camera (left) and real monitor camera.

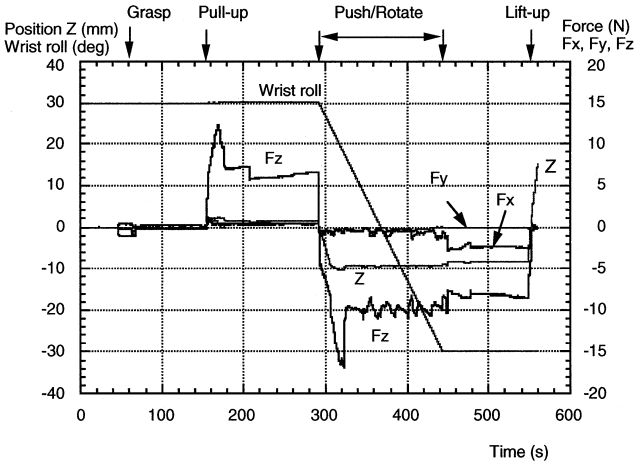

Fig. 17 Force and position data in sample removal.

firmly. We found that the force required to tear off the fastener was three times greater at the cold temperature in space than that at room temperature. Then, we improved software for optimizing the peel-off direction and employing a wobbling maneuver. Thus, the robot successfully performed the task, and the solar-cell sheet generated power and lit the LED.

We carried out a failure inspection for a stuck spherical part. We examined the cause by telesensing through teleteaching. The sensing strategy was interactively taught on the CG by dragging and dropping a virtual pipe that represented the hand center (see Fig. 7). The position of the hand was slightly changed step by step, and the force and angle of each finger were measured to identify the relationship between holding force and fine displacement. From the stiffness data we concluded that the cause is cold welding between the part and holder. The telesensing through teleteaching was very effective for examination and resolution of anomalies in space.

We also successfully carrried out wire hanging to the reel by means of teleoperation from the ground, employing a virtual operator function in onboard software.[11]

Conclusions

The concept of sensor-fused telerobotics using a multisensory hand was proposed for high-precision in-orbit servicing. A flight system was developed on the basis of the concept and tested on ETS-VII. It was efficiently operated from the ground through a space communication network. The main results of the space test are 1) the four-stage strategy of multisensor-based control was effective for in-orbit high-precision tasks, 2) telesensing through the multisensory hand satisfactorily resolved uncertainties of the work object/environment in space, and 3) a desktop ground operation system with a mouse-master device, a virtual hypercamera, and the teleteaching function provided a flexible and operator-friendly unified human/robot interface.

Acknowledgments

This project is promoted by the Ministry of Economy, Trade, and Industry/Institute for Unmanned Space Experiment Free Flyer of Japan. The author acknowledges the related staff. We also acknowledge National Space Development Agency of Japan for their development and operation of ETS-VII.

References

[1]Hirzinger, G., Brunner, B., Dietrich, J., and Heind, J., "Sensor-Based Space Robotics-ROTEX and Its Telerobotic Features," *IEEE Transactions on Robotics and Automation*, Vol. 9, No. 5, 1993, pp. 649–663.

[2]Kuwao, F., Motohashi, S., Hayashi, M., Matsueda, T., and Sato, N., "Dynamic Performance of Japanese Experiment Module Remote Manipulator System," *Proceedings of the International Symposium on Automation, Artificial Intelligence, Robotics and Automation in Space (i-SAIRAS) '97*, Tokyo, 1997, pp. 205–210.

[3]Rubinger, B., Fulford, P., Gregoris, L., Gosselin, C., and Laliberté, T., "Self-Adapting Robotic Auxiliary Hand (SARAH) for SPDM Operations on the International Space Station," *Proceedings of i-SAIRAS* [CD-ROM], Montreal, 2001.

[4]Borduas, H., Gossain, D., Kong, A., Quittner, E., and Shaffer, D., "Concept Design of the Special Purpose Dexterous Manipulator for the Space Station Mobile Servicing System," *Canadian Aeronautics and Space Journal*, Vol. 35, No. 4, 1989, pp. 197–204.

[5]Mugnuolo, R., "ASI Technology for Robotics Applications in Space," *Proceeding of i-SAIRAS*, [CD-ROM], Montreal, 2001.

[6]Skarr, S. B., and Ruoff, C. F., *Teleoperation and Robotics in Space*, Vol. 161, Progress in Astronautics and Aeronautics, AIAA, Washington, DC, 1994.

[7]Oda, M., "Engineering Test Satellite VII, Rendezvous, Docking and Space Robot Satellite," *Proceedings of i-SAIRAS'97*, 1997, pp. 59–62.

[8]Sheridan, T. B., *Telerobotics, and Human Supervisory Control*, MIT Press, Cambridge, MA, 1992.

[9]Machida, K., Toda, Y., and Iwata, Y., "Graphic Simulator Augmented Teleoperation System for Space Applications," *Journal of Spacecraft and Rockets*, Vol. 27, No. 1, 1990, pp. 64–69.

[10]Kubota, N., Ohno, M., Sakata, R., Machida, K., Tanie., K., and Akita, K., "Fexible Solar Cell Sheet Handling by a Three-finger Multisensory Hand," *Proceedings of the International Conference of Advanced Robotics (ICAR'99)*, Tokyo, 1999, pp. 425–430.

[11]Matsuhira, N., Asakura, M., Shinomiya, Y., Machida, K., Tanie, K., and Akita, K., "Wire Handling Experiment by Teleoperation of the Advanced Robotic Hand from the Ground," *Proceeding of ICAR'99*, Tokyo, 1999, pp. 431–436.

D. B. Spencer
Associate Editor